The role of IDH1 mutated tumour cells in secondary glioblastomas: an evolutionary game theoretical view

2011 Phys. Biol. 8 015016

(http://iopscience.iop.org/1478-3975/8/1/015016)

Phys. Biol. **8** (2011) 015016 (9pp) doi:10.1088/1478-3975/8/1/015016

The role of IDH1 mutated tumour cells in secondary glioblastomas: an evolutionary game theoretical view

David Basanta[1], Jacob G Scott[1], Russ Rockne[2], Kristin R Swanson[2] and Alexander R A Anderson[1]

[1] Integrated Mathematical Oncology, H Lee Moffitt Cancer Center and Research Institute, Tampa, FL 33612, USA

[2] Pathology and Applied Mathematics at the University of Washington, Seattle, WA 98104, USA

E-mail: david.basanta@kclalumni.net and jacob.scott@moffitt.org

Received 17 September 2010
Accepted for publication 10 January 2011
Published 7 February 2011
Online at stacks.iop.org/PhysBio/8/015016

Abstract

Recent advances in clinical medicine have elucidated two significantly different subtypes of glioblastoma which carry very different prognoses, both defined by mutations in isocitrate dehydrogenase-1 (IDH-1). The mechanistic consequences of this mutation have not yet been fully clarified, with conflicting opinions existing in the literature; however, IDH-1 mutation may be used as a surrogate marker to distinguish between primary and secondary glioblastoma multiforme (sGBM) from malignant progression of a lower grade glioma. We develop a mathematical model of IDH-1 mutated secondary glioblastoma using evolutionary game theory to investigate the interactions between four different phenotypic populations within the tumor: autonomous growth, invasive, glycolytic, and the hybrid invasive/glycolytic cells. Our model recapitulates glioblastoma behavior well and is able to reproduce two recent experimental findings, as well as make novel predictions concerning the rate of invasive growth as a function of vascularity, and fluctuations in the proportions of phenotypic populations that a glioblastoma will experience under different microenvironmental constraints.

1. Introduction

Our ability to tease apart pathologic differences in cancers began with microscope and differential staining and has progressed to the current age of molecular medicine. The mantra of clinical medicine in the molecular age is 'personalized medicine'—the hope that one day we will be able to perfectly understand each person's tumor at the molecular and mechanistic level in order to prescribe the perfect treatment. While we have made many advances in subtyping many different cancers and even designed molecularly targeted therapies, the results so far have been disappointing. One cancer that has remained particularly resistant to our therapies is glioblastoma multiforme (GBM), which carries a prognosis of less than a year and certain mortality.

It has been understood for several years that there are different subtypes of glioblastoma characterized by mutation pattern and cell of origin [1], but this knowledge has not altered our treatment strategy, only our ability to prognosticate outcome. That these subtypes all end up looking the same under the microscope and end up behaving very similarly as aggregates is an example of convergent evolution—genotypically different cells with similar phenotypic characteristics.

Most recently, two significantly different classes of glioblastoma have been identified which carry very different prognoses [2–4]. These two groups of glioblastoma are, for the most part, differentiated by mutations found in a single coding region of an enzyme involved in the Krebs cycle, isocitrate dehydrogenase 1 (IDH1). This mutation is present in the majority of secondary glioblastomas (sGBM) and low grade gliomas (LGGs), many of which progress to become

sGBMs. Recent published works have stressed different and sometimes opposing data concerning the effect of this mutation. Specifically, work published by Zhao *et al* [5] suggests that the major disruption of this mutation is metabolic in nature leading to dysregulation of the conversion of isocitrate to a-ketoglutarate (a-KG) and a concomitant increase in the hypoxia inducible factor-1α (HIF-1α) expression which is known to correlate with glioma progression [5]. In counterpoint is the work of Dang *et al* [6] which suggests that the levels of a-KG are unaffected, but that, instead, the mutation leads to a gain of function and the production of the onco-metabolite 2-hydroxyglutarate (2-HG). This byproduct has been linked to the formation and progression of brain tumors [7] in patients with the autosomal recessive disease L-2-hydroxyglataric aciduria, but the mechanism is unknown. Karcher *et al* [8] showed that the angiogenic cascade of primary glioblastoma is almost entirely dependent upon the vascular endothelial growth factor A (VEGF-A), while secondary glioblastoma depends equivalently on VEGF-A and the platelet-derived growth factor AB (PDGF-AB) suggesting that the neovascularization between the two subtypes is likely distinct.

These differences, while striking, have not yet made an impact on the treatment of sGBM, nor have they allowed for a consensus on the underlying mechanistic differences stemming from these genetic changes. One significant assumption that allows us to gain insight into these differences is that excessive production of angiogenic factors can lead to a vascular response that is far from optimal—with hallmarks of disordered vasculature being tortuous, ineffective and leaky vessels [9]. This has a direct implication for the IDH1 mutant sGBM, since it has been suggested that this mutation enhances the angiogenesis-inducing abilities of these tumors through regulation of HIF-1α. This, in conjunction with phenotypes that actively promote vascular formation (e.g. hypoxic cells), leads us to the hypothesis that IDH1 mutant sGBM, whilst good at recruiting vasculature, the functionality of this vasculature will critically depend on the interactions between the multiple phenotypes that makeup the tumor population. We use evolutionary game theory (EGT) as our modeling tool to investigate how interactions between distinct tumor phenotypes (relevant to sGBM) affect cancer progression.

In this paper we aim to integrate recent experimental and clinical insights into a theoretical model to gain deeper understanding of IDH1 mutated sGBM. In order to do that, we developed an EGT model of the interactions between four tumor phenotypes that we believe characterize sGBM and the role of IDH-1 as it relates to angiogenesis, a hallmark of this disease. The EGT-derived replicator equations show that vascularization affects cancer progression in a way that accelerates the emergence of invasive phenotypes. These results are consistent with clinical imaging and suggest that angiogenesis could play a major role in the dominance of invasive glycolytic phenotypes in other types of cancer.

2. An evolutionary game theory model

EGT is a mathematical tool that began in the social and economic sciences with the aim to understand how the interactions between different entities, called players, affect the outcome of a game [10–12]. EGT is also considered to be a promising tool in which to frame oncological problems [13]. With the new emphasis on cancer at the phenotypic level [14, 15], the suitability of mathematical tools, such as EGT, that focus on cell–cell interactions has been made more relevant.

In EGT the behavior of the players is not assumed to be based on rational payoff maximization, but it is thought to be shaped by trial and error—adaptation through natural selection or individual learning [16]. In the context of the evolution of populations there are two game theory concepts that have to be interpreted in a different light than in traditional game theory. First, a strategy is not a deliberate course of action but a phenotypic trait. The payoff is Darwinian fitness, that is, average reproductive success. Secondly, the players compete or cooperate to become a larger share of the population [11].

Early tumors are characterized by rapidly proliferating cells that have become independent from the microenvironment in regard to growth. It is also well known that tumor cells in gliomas are more motile than in solid tumors with as many as half of the patients having microscopic invasion of glioblastoma cells in the contralateral hemisphere at diagnosis [17]. We assume that the IDH1 mutants can emerge from the rapidly proliferating population or from the motile population. Thus, our model hypothesizes a tumor composed of four glioma cell phenotypes: autonomous growth (AG), invasive (INV), glycolytic (GLY) and a hybrid phenotype which is both invasive and glycolytic (INV-GLY). Only the last two types are assumed to have the IDH1 mutation. These phenotypes could represent cells with any number of specific genetic mutations, but in this model only the phenotype will be considered. It is also important to realize that these labels are broad categorizations of the phenotypes and that the INV phenotype is not constantly on the move but just more likely to migrate than the AG phenotype.

In our previous paper we described a simpler but similar model [18], where we examined the interactions between three cell phenotypes, AG, INV, and GLY, in order to understand the relationship between invasion and glycolytic fractions. The model described in this paper builds on the strengths of the previous one and extends it with the addition of a fourth phenotype, INV-GLY, and a parameter (α) that allows us to examine the effects of angiogenesis within the context of sGBM. The relative costs and benefits of how cells with different phenotypes interact with each other and with the microenvironment are defined in the payoff table 1. We utilize the same parameters as our previous model (c, k and n) [18] and a new one (α) which represents the benefit of vascularity with regard to proliferation. The parameter c represents the cost of motility for the phenotypes capable of moving (INV and INV-GLY), which is assumed to be very low in glioma when compared with solid cancers like carcinomas. This fitness cost can be viewed, among other things, as an opportunity cost that

Table 1. The four phenotypes in the game are autonomous growth (AG), invasive (INV), glycolytic (GLY) and invasive glycolytic (INV-GLY). The base payoff in a given interaction is r and the cost of moving to another location with respect to the base payoff is c. The fitness cost of acidity is n and k is the fitness cost of having a less efficient glycolytic metabolism. The benefits from having access to the vasculature as a result of angiogenesis are reflected by the parameter α.

	AG	INV	GLY	INV-GLY
AG	$\frac{1}{2}+\frac{\alpha}{2}$	1	$\frac{1}{2}-n+\alpha$	$\frac{1}{2}-n+\alpha$
INV	$1-c$	$1-\frac{c}{2}$	$1-\frac{c}{3}$	$1-\frac{c}{3}$
GLY	$\frac{1}{2}-k+n+\alpha$	$1-k+\frac{\alpha}{2}$	$\frac{1}{2}-k+\frac{\alpha}{4}$	$1-k+\frac{\alpha}{2}$
INV-GLY	$\frac{1}{2}-k+n+\alpha$	$1-k+\frac{\alpha}{2}$	$1-\frac{c}{3}-k+\frac{\alpha}{2}$	$1-k-\frac{c}{6}+\frac{\alpha}{2}$

Table 2. List of variables used by the model.

Value	Affected phenotypes	Meaning
c	INV, INV-GLY	Cost of motility
k	GLY, INV-GLY	Cost having a glycolytic metabolism
n	AG, INV	Cost of living in an acid microenvironment
α	AG, GLY, INV-GLY	Benefit from angiogenesis

moving cells incur since they cannot proliferate whilst moving [19, 20] or as the cost for degrading and detaching from the extra cellular matrix. The parameter k represents the cost of utilizing glycolysis as opposed to the more efficient oxidative phosphorylation. The parameter n represents the penalty that cells suffer for living in an acidic environment created by the glycolytic cells. GLY cells will suffer this penalty less as they are adapted to live in acidic environments. The parameter α represents the benefit of the surrounding vasculature. One way of envisioning variations in α is the increase in oxygen and nutrients resulting from an optimized vascularization resulting from the release of HIF-1α and downstream proteins. Table 2 lists all model variables. These variables are normalized and assumed to be in the range [0:1].

The payoff table 1 assumes that non-motile phenotypes (GLY and AG) will share existing resources with the cells they interact with, whereas motile phenotypes can chose whether to stay or move. In the case of INV cells, they will always move and leave existing resources for the cell it is interacting with unless the interaction happens with another INV cell, in which case one of the INV stays. INV-GLY cells behave as GLY cells when interacting with non-glycolytic cells (AG and INV) but move in response to the acidification of the environment.

One important difference with the previous model is that angiogenesis is now possible for cells, once they reach a critical mass, to produce enough angiogenic factor to benefit from added vasculature. As a result of HIF-1α being produced, resources needed for sustained tumor growth are provided by newly formed vasculature. The model assumes that glycolytic cells (GLY and INV-GLY), having the IDH-1 mutation, produce more of this angiogenic factor. On the other hand, cells that are moving (not just capable of motility but stationary at a given time) do not produce significant HIF-1α. Furthermore, we assume that whereas too little HIF-1α leads to insufficient vascularization, too much of it can lead to leaky or otherwise defective vascularization [9]. This is shown in the table by the fact that AG cells interacting with other AG cells (assumed to produce only moderate amounts of HIF-1α) receive a benefit of $\frac{\alpha}{2}$ from the moderate angiogenic vasculature. On the other hand, AG cells interacting with GLY cells produce, in combination, an optimal amount of HIF-1α and obtain in return the total benefit derived from functioning vascularity (α). Finally, as IDH-1 mutant GLY cells proliferate producing excessive amounts of HIF-1α, the benefit of angiogenesis is a reduced $\frac{\alpha}{4}$, consistent with the angiogenic vasculature being leaky and inefficient in this case.

Another notable difference with the previous model is that the cost of motility is assumed to be smaller in the presence of acid-producing glycolytic phenotypes. This is represented by a cost of motility $\frac{c}{3}$ and represents the acid-mediated invasion [21–23] of glioma cells throughout the brain, particularly along the myelinated neuronal axons in the white matter of the brain along which glioma cells are known to quickly invade [24, 25]. This reduced cost of motility also quantifies and models the generally invasive characteristics of gliomas which are well known for their diffuse invasion that has been quantified in human gliomas to be at rates suggesting significant motility on the time scale of hours [25, 26].

From the payoff table (table 1) it is possible to derive replicator equations that describe the change in the tumor populations over time. The fitness of any given population will depend on the results of the interactions with other phenotypes. If the proportion of INV phenotypes is p_i, the proportion of GLY ones is p_g and the proportion of INV-GLY is p_{ig}, then the fitness of an AG cell is

$$\begin{aligned} W(\mathrm{AG}) &= (1-p_i-p_g-p_{ig})\left(\frac{r}{2}+\frac{\alpha}{2}\right)+p_i(r) \\ &\quad + p_g\left(\frac{r}{2}-n+\alpha\right)+p_{ig}\left(\frac{r}{2}-n+\alpha\right) \\ &= \frac{r+\alpha}{2}+p_i\frac{r-\alpha}{2}+(p_g+p_{ig})\left(\frac{\alpha}{2}-n\right). \end{aligned} \tag{1}$$

Similarly, the fitness of INV cells is

$$\begin{aligned} W(\mathrm{INV}) &= (1-p_i-p_g-p_{ig})(r-c)+p_i\left(r-\frac{c}{2}\right) \\ &\quad + p_g\left(r-\frac{c}{3}\right)+p_{ig}\left(r-\frac{c}{3}\right) \\ &= r-c+p_i\frac{c}{2}+p_g\frac{2}{3}c+p_{ig}\frac{2}{3}c. \end{aligned} \tag{2}$$

The GLY cell fitness is

$$\begin{aligned} W(\mathrm{GLY}) &= (1-p_i-p_g-p_{ig})\left(\frac{r}{2}-k+n+\alpha\right) \\ &\quad + p_i\left(r-k+\frac{\alpha}{2}\right)+p_g\left(\frac{r}{2}-k+\frac{\alpha}{4}\right)+p_{ig}\left(r-k+\frac{\alpha}{2}\right) \\ &= \left(\frac{r}{2}-k+n+\alpha\right)+p_i\left(\frac{r-\alpha}{2}-n\right) \\ &\quad - p_g\left(n+\frac{3}{4}\alpha\right)+p_{ig}\left(\frac{r-\alpha}{2}-n\right), \end{aligned} \tag{3}$$

and finally INV-GLY is defined as

$$\begin{aligned} W(\mathrm{INV\text{–}GLY}) &= (1-p_i-p_g-p_{ig}) \\ &\quad \times\left(\frac{r}{2}-k+n+\alpha\right)+p_i\left(r-k+\frac{\alpha}{2}\right) \\ &\quad + p_g\left(r-\frac{c}{3}-k+\frac{\alpha}{2}\right)+p_{ig}\left(r-k-\frac{c}{6}+\frac{\alpha}{2}\right) \end{aligned}$$

$$= \left(\frac{r}{2} - k + n + \alpha\right) + p_i\left(\frac{r-\alpha}{2} - n\right) + p_g\left(\frac{r-\alpha}{2} - \frac{c}{3} - n\right) + p_{ig}\left(\frac{r-\alpha}{2} - \frac{c}{6} - n\right). \quad (4)$$

The average fitness ($\bar{W}$) of the entire population is given by

$$\bar{W} = (1 - p_i - p_g - p_{ig})W(\mathrm{AG}) + p_i W(\mathrm{INV}) + p_g W(\mathrm{GLY}) + p_{ig} W(\mathrm{INV} - \mathrm{GLY}). \quad (5)$$

From these expressions it is possible to derive the discrete replicator equations that describe, using the absolute fitness of each of the populations, how the different phenotypic populations change over time [16]. The proportion of a cellular population in the model at a given time t will depend not only on its own fitness (W) but also on the fitness of the other cell populations. If the fitness of a phenotype X, $W(X)$, is higher than the average fitness of all the phenotypes combined ($\bar{W}$), then the proportion of that phenotype will increase in $t + 1$, for as long as the reasons that keep the phenotype relatively fit remain. The replicator equations are defined as follows:

$$p_{i_{t+1}} = p_{i_t}\frac{W(\mathrm{INV})}{\bar{W}}, \quad p_{g_{t+1}} = p_{g_t}\frac{W(\mathrm{GLY})}{\bar{W}}, \quad p_{ig_{t+1}} = p_{ig_t}\frac{W(\mathrm{INV} - \mathrm{GLY})}{\bar{W}}. \quad (6)$$

It is important to bear in mind that the time steps do not represent a specific measure of time.

3. Results

Since IDH1 has been implicated in the control of the angiogenic cascade, we began our exploration of the parameter space focused on the variable α which can be thought of as a surrogate for vascularity or vascular fitness. In these simulations, we measured the glycolytic fraction (GLY + INV-GLY) as these cells are able to be approximated clinically with imaging (MR spectroscopy or FDG-PET) and because earlier work has suggested that emergence of the glycolytic phenotype is a prerequisite for the emergence of invasion [18, 27]. We found that in the glioma relevant areas of the parameter space (with relatively low cost of glycolysis, k, and motility, c), the pure GLY cells never composed a significant fraction of the total glycolytic proportion after invasion emerged. And since invasion is a definitive component of all human gliomas, we chose to concentrate on measuring the proportion of the population composed of INV-GLY cells.

To explore this relationship, we ran the replicator equations for 5000 time steps for 1000 values (in increments of 0.001 between 0 and 1) of α and c (cost of motility) and measured the proportion of INV-GLY cells for a number of k, n (cost of acidification) value pairs. Four representative examples of such plots are shown in figure 1. As the cost of glycolysis (value of k) increases, the proportion of the parameter space in which INV-GLY cells dominate shrinks. Through all values, a diagonal relationship emerges in which we see that matched extreme values of α and c select against INV-GLY cells. In the most glioma relevant plots (in which the cost of glycolysis, k, and motility, c, are relatively low) we see a strong dependence of the INV-GLY fraction on α for all values of c. It is worth noting that for higher values of k, parts of the parameter space show discontinuities that result from the fact that purely GLY cells are very competitive with INV-GLY for those values of c and α and, given the oscillations that characterize the population dynamics, the cutout time step can show either GLY or INV-GLY dominance. A better view of this would be that in that area of the parameter space, coexistence of those two phenotypes should be expected.

Since the emergence of the INV-GLY phenotype may be considered as a late stage event in glioma progression, we next explored the speed at which the INV-GLY cells dominated the entire tumor population. To do this we ran simulations at specific value pairs of k and n and varied c and α through all possible values. Figure 2 shows four plots with escalating k and n pairs matched to figure 1. We changed n at the same rate as k as the cost of living in an acid environment has to be higher than the cost of glycolysis for glycolytic phenotypes to emerge in the tumor. To measure the speed of progression, we subtracted the number of time steps it took for the tumor to reach 50% INV-GLY from 1000 (the maximum number of time steps the simulations were evaluated). So, a tumor with a speed of 999 took only one time step to reach INV-GLY dominance, while a tumor with a speed of 0 never achieved this dominance. The diagonal relationship that emerged in figure 1 again appears in these plots, with matched extreme c and α values having a speed of 0. This is somewhat expected, based on the results given in figure 1, since these tumors do not have a large proportion of INV-GLY cells. There are some notable areas of apparent discordance which can be misleading due to an artifact of our endpoint (e.g. in the $k = 0.2$ plots, the low α, high c portion of the plot has a very high speed value but a very low INV-GLY fraction, cf figures 1 and 2). While in this portion of the parameter space the INV-GLY proportion does indeed rapidly gain the majority proportion (high speed), it does not end up becoming winning at the end of the game (dynamic that is observed in data not shown).

While these plots have given us a big picture for understanding the behavior of the model, we have endeavored to understand the specific case of sGBM, and therefore a more rigorous exploration of the relevant area of the parameter space was warranted. Physiologically, the brain is always given precedence in the case of sugar supply, so the cost of glycolysis (k) is relatively low. It is well known that gliomas are extremely motile tumors, which would suggest a low c. We have shown that the behavior of the tumor is highly dependent upon α, so we chose to explore the dynamics of changing α on a tumor with $k = 0.1$, $c = 0.1$ and $n = 0.2$ (figure 3, control row). What we found was a strong dependence on α, not only on the temporal development of the different phenotypes in the tumor, but also on the overall outcome. Specifically, we observed that at low levels of α, the INV cells dominated, while increasing levels of α not only caused the game to change in favor of the INV-GLY cells but also sped up this outcome. These outcomes from our EGT model are consistent with observed behavior in LGG and sGBM tumors: LGGs do not

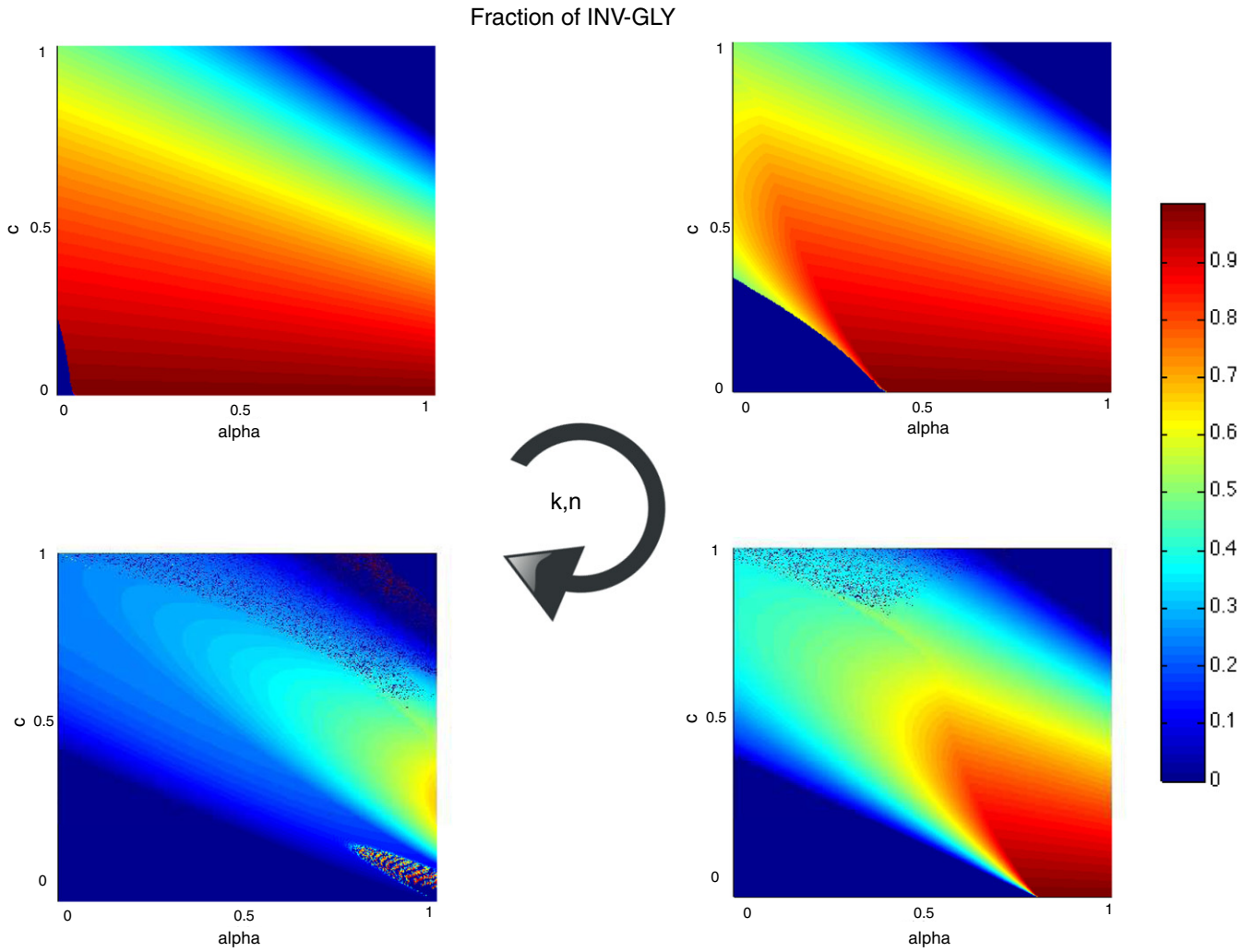

Figure 1. The fraction of INV-GLY cells after 5000 time steps as we increase the cost of glycolysis ($k = 0.01$, 0.1, 0,2 0.3) and acidity ($n =$ 0.02, 0.2, 0.3 and 0.4). The heatmap (from dark blue signifying low, to dark red signifying high) represents the proportion of INV-GLY cells. High values of α select for INV-GLY phenotypes and both extremely low and extremely high values of c select against it (by promoting pure INV in the former and pure GLY in the latter). As the cost of glycolysis increases, even as the benefit of acidifying the environment increases, the proportion of INV-GLY cells is reduced.

need new vasculature to survive and are capable of co-opting the existing vasculature in the brain for long periods of time, leading to a prognosis of decades. LGGs that do progress to become sGBMs outgrow the native nutrient supply in the brain. The connection to the IDH1 mutation that makes a distinction between primary and secondary GBM lies in the promotion of the glycolytic phenotype and suggests the hypothesis that primary GBM may differ from sGBM only in the rate at which they progress from a less malignant lesion. Specifically, the rate of progression may be so rapid in some primary GBM that by the time they are detected they have already become sGBM. Furthermore, figure 3 shows that the steady state is dependent on the value of α and that when this changes (as it is the case in the second and third row in figure 3), the dynamics of the tumor could change in ways that could reverse previous trends. Anti-angiogenics (like VEGF-inhibitor bevacizumab) are currently used clinically in an attempt to tame the angiogenic vasculature found within gliomas [28]. The second row of figure 3 shows an investigation of the effect of treatment with anti-angiogenics on our EGT-derived virtual gliomas. We iterated the game for the parameter values found in figure 3(a)–(c), and at time step 600 we imposed a decrease in alpha (vascular fitness) to correspond to the anti-angiogenic treatment effect in figures 3(d)–(f). In all cases, there is a significant selection for the INV phenotype and away from GLY and GLY-INV phenotypes. Further, the total proportion of the tumor that is invasive (INV+ GLY-INV) increases with the treatment with anti-angiogenic. These results are strikingly similar to those observed clinically in which there is a dramatic increase in invasion of these tumors. Figure 4 illustrates the case of GBM treated with bevacizumab in which the glycolytic fraction of the tumor is decreased (nodular tumor in figure 4(C) decreases on FDG-PET as shown in figure 4(F)) and the recurrent tumor exhibits a dramatic invasion across the corpus callosum (figure 4(E)). Further, the simulations in figures 3(d)–(f) suggest a testable prediction that sGBMs treated with

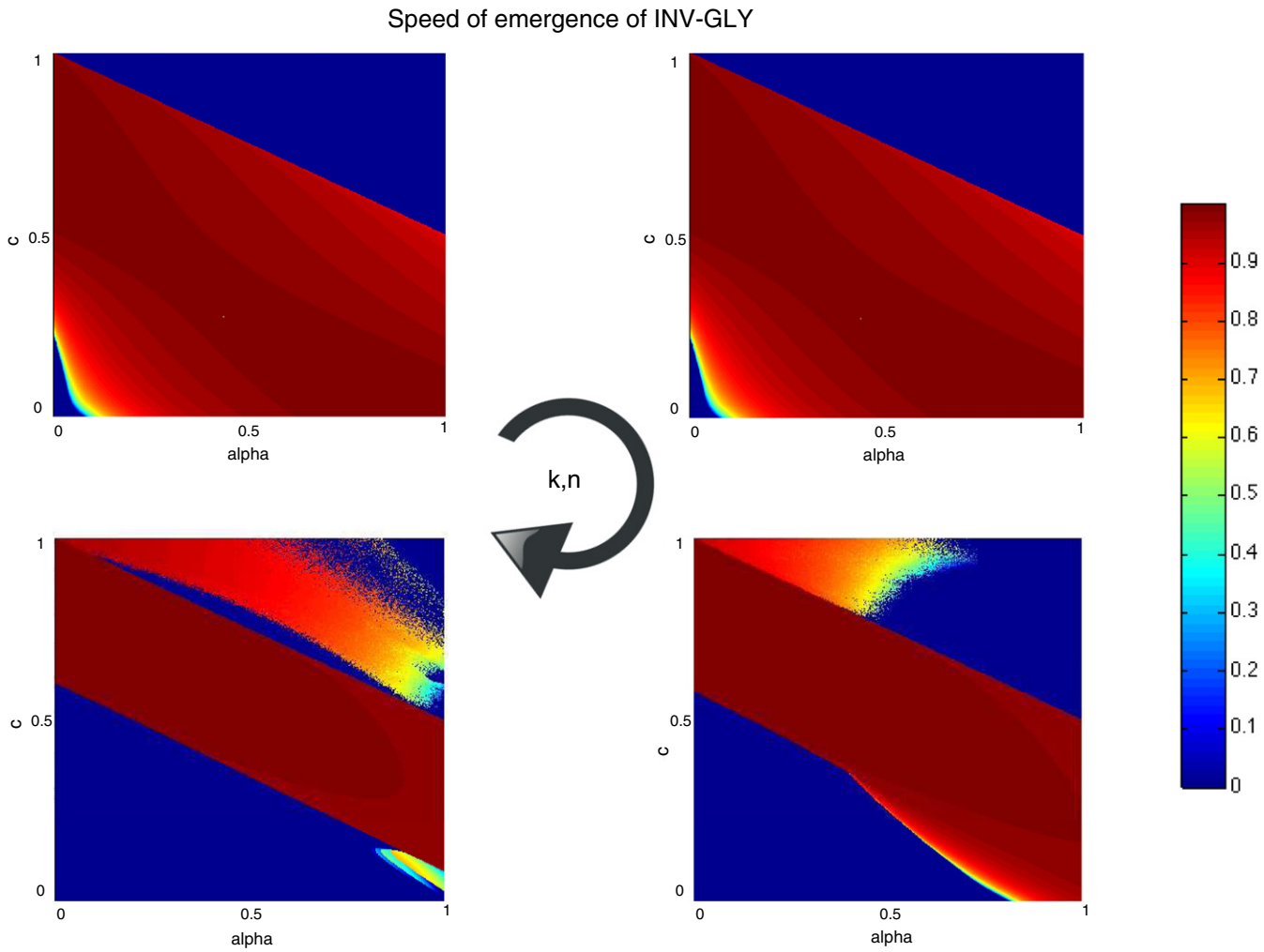

Figure 2. The speed of progression toward the malignant invasive glycolytic phenotype as we increase the cost of glycolysis ($k = 0.01$, 0.1, 0,2 0.3) and acidity ($n = 0.02$, 0.2, 0.3 and 0.4). The heatmap (from dark blue signifying low, to dark red signifying high) represents the speed. This is measured between 0 and 999, with the former implying that a majority of INV-GLY is never achieved and the latter implying that this majority is reached after only one time step.

anti-angiogenics will become dominated by invasive phenotypes that are less likely to be glycolytic.

4. Discussion

The advent of the molecular age has enabled the possibility of truly personalized treatment of cancer. Increasingly we are identifying important mutations that confer specific advantages to tumors, and yet only in a handful of situations have we been able to capitalize on this information. Much work has been done of late in glioblastoma to understand the specific genetic pathways at work in this disease. Most recently, the mutation in IDH1 has been identified as a marker of good prognosis for glioblastomas, but the mechanism for this has yet to be elucidated. In this work we have attempted to understand this prognostic change by building and exploring a mathematical model that takes into consideration the recent developments surrounding this mutation. We have chosen EGT to explore this question because of its elegant simplicity and because of its ability to tease apart interacting tumor populations at the phenotype level.

The first test of any model should be to ensure that it can recapitulate known behaviors. On this point our model succeeds on a number of fronts. We found that increasing the level of benefit of angiogenesis (α) in glioma relevant areas of the parameter space corresponded with an increased speed of progression, marked by a quicker arrival at higher glycolytic fractions (figure 2). This result is nicely corroborated in a clinical trial reported by Kruer *et al* [29] that showed that patients with hypermetabolic tumors as imaged using fluorodeoxyglucose (^{18}F) FDG-PET had a significantly quicker time to clinical progression (33 versus 52.3 months). While this result is somewhat intuitive, another aspect of the model behavior is less so, and could have tempered some of the fervor toward anti-angiogenic therapies when they were first introduced. We find that when we reduce the benefit of angiogenesis (reduce α) the imaging surrogate for the glycolytic phenotype, FDG-PET avidity, is blunted, and the fraction of cells displaying the invasive phenotype is promoted. This has recently been well documented by both imaging and histologic studies [30] and serves as an explanation for the

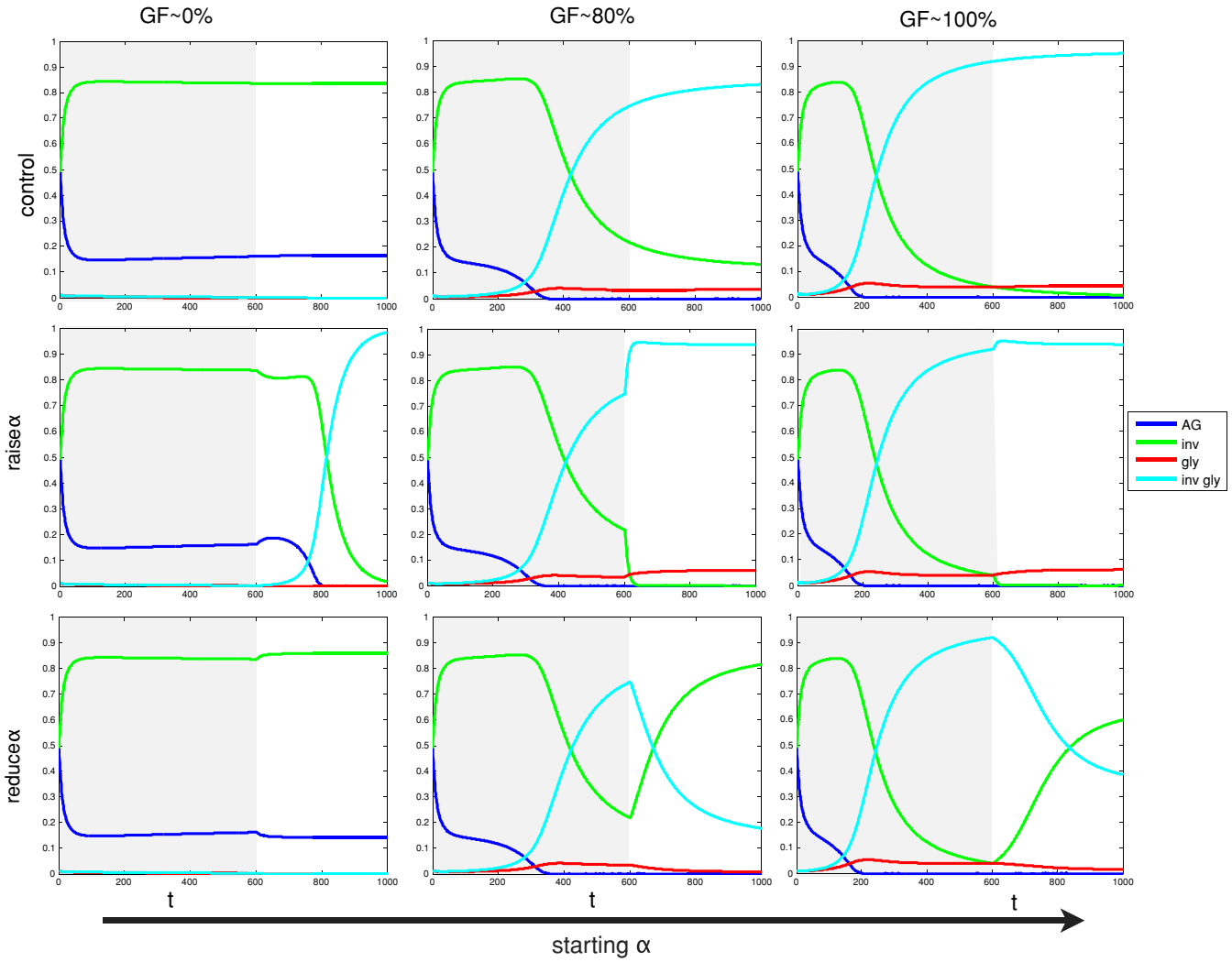

Figure 3. Plot of $k = 0.1$, $n = 0.2$, $c = 0.1$ and $\alpha = 0.3, 0.32, 0.35$. The first panel shows two interesting dynamics: with increasing benefit of vasculature (increasing α), we see a more rapid progression as well as a higher overall proportion of cells with the GLY phenotype. Also, decreasing α promotes the INV phenotype (stars) which is recapitulated in recurrent glioblastoma after bevacizumab treatment. The two panels below the control one show what happens after bevacizumab has been administered after 600 time steps without assuming whether the main effect would be a normalization of the angiogenic vasculature (which would increase α, shown in the second row) or the reduction of the existing vasculature (which would have a negative effect on α, shown in the third row).

changes that we see in glioblastoma patients after failure of bevacizumab (a monoclonal antibody to VEGF-α).

The recapitulation of known behaviors allows some measure of confidence in our model and gives some credence to predictions that the model can make. Now we can begin to make observations about the mechanisms driving the behaviors that were, otherwise, obscured by the biological complexity. A recurring theme observed in the time-dependent behavior of our model suggests an underlying mechanism driven by interactions between different phenotypes. Specifically, the emergence of the invasive phenotypes is always preceded by a rise in the glycolytic fraction. This rise in the glycolytic fraction is preceded by an overgrowth of AG cells. Mechanistically, this could be explained as follows: AG cells outgrow the resources available to them in their local environment causing, among other things, hypoxia. This hypoxia initiates the angiogenic cascade and begins to allow the GLY cells to outcompete the AG cells. Once the GLY cells grow into a viable proportion, the damage that they do to the local environment with their excessive acid production begins to promote the benefit of cells that can move to a new place (INV). We see this sequence reproduced in nearly all areas of the parameter space, and certainly in all the areas that are relevant to glioma. Further, these results agree nicely with earlier work done by this group suggesting that the glycolytic phenotype is necessary to bring about the emergence of invasion [18].

In addition to this sequence, there was an interesting dynamic that emerged in some areas of the parameter space. Figure 5 shows an example of two types of oscillatory behavior that our model can produce. Even though neither manage to sustain the oscillations for too long, they both exhibit dominate alternating oscillations of high AG giving way to high INV. In figure 5(*a*) the INV-GLY phenotype is an intermediary between these and eventually aids in the emergence of the INV population as the single dominant phenotype. Whilst

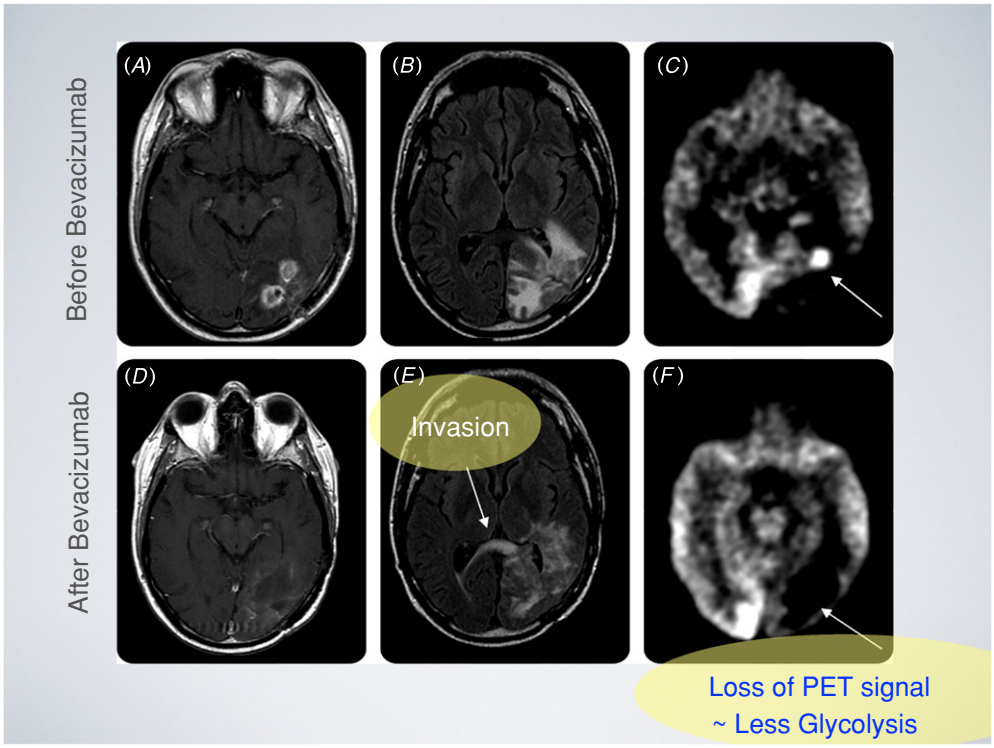

Figure 4. In this series of images, adapted from Iwamoto *et al* [30] we see three images from the same patient before and after treatment with anti-angiogenic therapy, in this case bevacizumab. The top three images, representative of high alpha, show high glycolysis and low invasion. After treatment with bevacizumab, we see a reduction in glycolytic fraction (blunting of FDG-PET avidity) and the promotion of invasion, as predicted by our model.

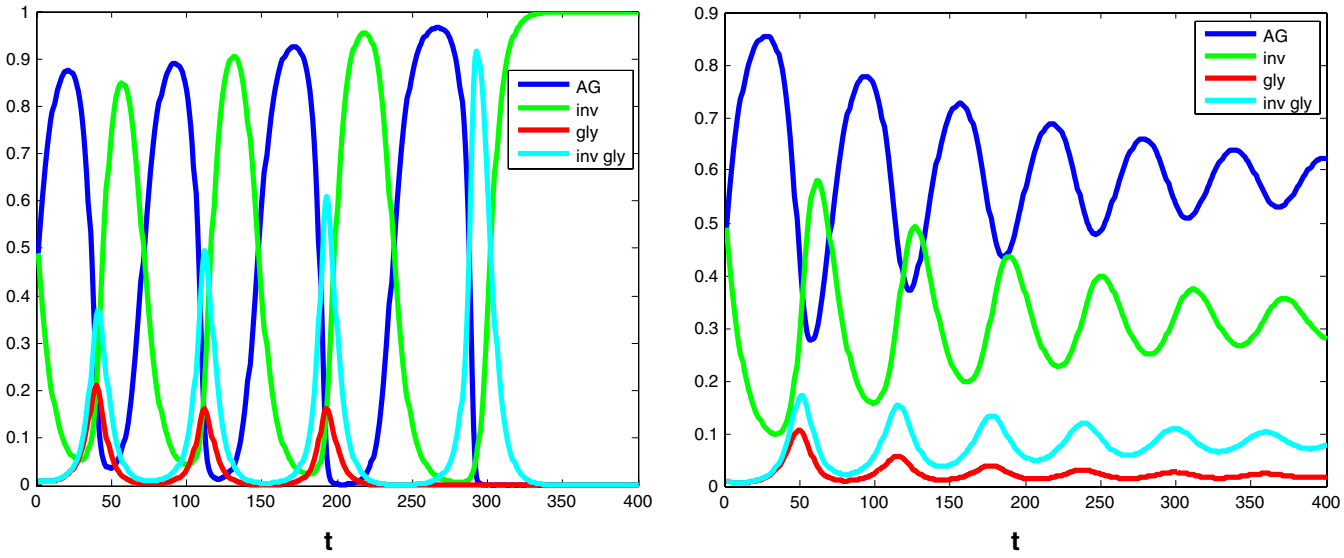

Figure 5. Two examples of oscillations that are characteristic of some of the simulations with the replicator equations. In both cases these oscillations are transient, leading to a steady state characterized by non-glycolytic cells. In the first scenario, with high costs of motility and glycolysis (k and $c = 0.4$) and $\alpha = 0.35$, the steady state is dominated by purely invasive cells and the oscillations are characterized by dominance of AG cells which leads to a surge in glycolytic cells that selects for invasive phenotypes. In the second scenario (k and $c = 0.4$) the slightly smaller value of α (0.25) means that glycolytic cells never emerge in large enough numbers to help purely invasive cells dominate the tumor population.

there is no evidence that such oscillations truly occur in real tumors, it is an intriguing prediction that is also hinted at in the sequence we discussed above, i.e. the metabolic activity of the tumor may have a cyclic nature that ultimately leads to emergence of a purely invasive population.

In figures 1 and 2 we explored the effect of varying k, the cost of glycolysis, on the steady-state INV-GLY fraction and the speed at which INV-GLY cells reach a majority of the tumor population. This change in k could represent changes in the levels of available substrate for glycolysis. It is possible

that the value of k could change in a cyclical fashion as tumors grow beyond their carrying capacity (increasing k) or produce new vessels (which would decrease k). We found that the proportion of INV-GLY phenotypes is sensitive to changes in k and that, therefore, the proportion of INV-GLY cells could change over periods of time as k varies up and down.

We have presented an evolutionary game theoretical model weaving together recent discoveries concerning the underlying biology of sGBM which nicely recapitulates the known behavior of this disease and further serves to elucidate some underlying mechanistic processes at the phenotype scale. The newest hope on the horizon for glioma therapeutics lies in new drugs targeting proteins necessary for invasion. These drugs would serve to affect our model by artificially increasing the cost of motility and are therefore testable with our construct. Future work with this model will center around perturbations with these novel therapeutics by varying order, combinations and 'dose' allowing for testable clinical hypotheses. Additionally, other investigations with this EGT model include adapting the model parameter r that represents the benefit from the fitness of the environment to make a clear distinction between gray and white matter regions in the brain as well as the differential cost of motility in each (c). Although the game is not spatial, these aspects may be incorporated by comparing multiple games and varying these parameters such that they represent gliomas originating in 'primarily' gray or white matter regions of the anatomy, as well as regions of interface between the tissue types. Future work could also include making the model more qualitative which would allow a better validation of the model using image-driven parameter estimation [31].

Acknowledgment

This work was supported in part by NIH 1 U54 CA143970-01.

References

[1] Wen P Y and Kesari S 2008 Malignant gliomas in adults *N. Engl. J. Med.* **359** 492–507
[2] Parsons D W *et al* 2008 An integrated genomic analysis of human glioblastoma multiforme *Science* **321** 1807–12
[3] Nobusawa S, Watanabe T, Kleihues P and Ohgaki H 2009 Idh1 mutations as molecular signature and predictive factor of secondary glioblastomas *Clin. Cancer Res.* **15** 6002–7
[4] Yan H *et al* 2009 Idh1 and Idh2 mutations in gliomas *N. Engl. J. Med.* **360** 765–73
[5] Zhao S *et al* 2009 Glioma-derived mutations in IDH1 dominantly inhibit IDH1 catalytic activity and induce hif-1alpha *Science* **324** 261–5
[6] Dang L *et al* 2010 Cancer-associated IDH1 mutations produce 2-hydroxyglutarate *Nature* **465** 966
[7] Aghili M, Zahedi F and Rafiee E 2009 Hydroxyglutaric aciduria and malignant brain tumor: a case report and literature review *J. Neurooncol.* **91** 233–6
[8] Karcher S, Steiner H H, Ahmadi R, Zoubaa S, Vasvari G, Bauer H, Unterberg A and Herold-Mende C 2006 Different angiogenic phenotypes in primary and secondary glioblastomas *Int. J. Cancer* **118** 2182–9
[9] Jain R K, Tomaso E di, Duda D G, Loeffler J S, Sorensen A G and Batchelor T T 2007 Angiogenesis in brain tumours *Nat. Rev. Neurosci.* **8** 610–22
[10] von Neumann J and Morgernstern O 1953 *Theory of Games and Economic Behaviour* (Princeton, NJ: Princeton University Press)
[11] Sigmund K and Nowak M 1999 Evolutionary game theory *Curr. Biol.* **9** 503–5
[12] Nowak M 2006 *Evolutionary Dynamics* (Cambridge, MA: Belknap)
[13] Gatenby R and Maini P 2003 Cancer summed up *Nature* **421** 321
[14] Hanahan D and Weinberg R 2000 The hallmarks of cancer *Cell* **100** 57–70
[15] Hahn W C and Weinberg R 2002 Rules for making human tumor cells *N. Engl. J. Med.* **347** 1593–603
[16] Smith J M 1982 *Evolution and the Theory of Games* (Cambridge: Cambridge University Press)
[17] Matsukado Y, Maccarty C S and Kernohank J W 1961 The growth of glioblastoma multiforme (astrocytomas, grades 3 and 4) in neurosurgical practice *J. Neurosurgery* **18** 636–44
[18] Basanta D, Simon M, Hatzikirou H and Deutsch A 2008 Evolutionary game theory elucidates the role of glycolysis in glioma progression and invasion *Cell Prolif.* **41** 980–7
[19] Giese A, Loo M, Tran N, Haskett S W and Berens M E 1996 Dichotomy of astrocytoma migration and proliferation *Int. J. Cancer* **67** 275–82
[20] Giese A, Bjerkvig R, Berens M E and Westphal M 2003 Cost of migration: invasion of malignant gliomas and implications for treatment *J. Clin. Oncol.* **21** 1624–36
[21] Gatenby R, Gawlinski E, Gmitro A, Kaylor B and Gillies R 2006 Acid-mediated tumor invasion: a multidisciplinary study *Cancer Res.* **66** 5216–23
[22] Gatenby R A and Gawlinski E T 2003 The glycolytic phenotype in carcinogenesis and tumor invasion *Cancer Res.* **63** 3847–54
[23] Gatenby R A and Gillies R J 2004 Why do cancers have high aerobic glycolysis? *Nat. Rev. Cancer* **4** 891–9
[24] Swanson K R, Alvord E C and Murray J D 2000 A quantitative model for differential motility of gliomas in grey and white matter *Cell Prolif.* **33** 317–29
[25] Harpold H L P, Ellsworth C A Jr and Swanson K R 2007 The evolution of mathematical modeling of glioma proliferation and invasion *J. Neuropathol. Exp. Neurol.* **66** 1–9
[26] Wang C H *et al* 2009 Rognostic significance of growth kinetics in glioblastoma: novel insights from combining serial mr imaging with a bio-mathematical model for glioma growth and invasion *Cancer Res.* **69** 9133–40
[27] Gatenby R and Gillies R J 2004 Why do cancers have high aerobic glycolysis? *Nat. Rev. Cancer* **4** 891–9
[28] Raizer J J *et al* (North American Brain Tumor Consortium) 2010 A phase II trial of erlotinib in patients with recurrent malignant gliomas and nonprogressive glioblastoma multiforme postradiation therapy *Neuro Oncol.* **12** 95–103
[29] Kruer M C, Kaplan A M, Etzl M M Jr, Carpentieri D F, Dickman P S, Chen K, Mathieson K and Irving A 2009 The value of positron emission tomography and proliferation index in predicting progression in low-grade astrocytomas of childhood *J. Neurooncol.* **95** 239–45
[30] Iwamoto F M, Abrey L E, Beal K, Gutin P H, Rosenblum M K, Reuter V E, DeAngelis L M and Lassman A B 2009 Patterns of relapse and prognosis after bevacizumab failure in recurrent glioblastoma *Neurology* **73** 1200–6
[31] Hogea C, Davatzikos C and Biros G 2008 An image-driven parameter estimation problem for a reaction-diffusion glioma growth model with mass effects *J. Math. Biol.* **56** 793–825